Solar Energy Materials & Solar Cells 95 (2011) 2540–2544

Contents lists available at ScienceDirect

Solar Energy Materials & Solar Cells

journal homepage: www.elsevier.com/locate/solmat

Letter

Efficiency enhancement of the poly-silicon solar cell using self-assembled dielectric nanoparticles

C.K. Huang [a], H.H. Lin [a], J.Y. Chen [a], K.W. Sun [a,*], W.-L. Chang [b]

[a] Department of Applied Chemistry, National Chiao Tung University, Hsinchu, Taiwan
[b] Green Energy & Environment Research Laboratories (GEL), Industrial Technology Research Institute (ITRI), Hsinchu, Taiwan

ARTICLE INFO

Article history:
Received 16 December 2010
Accepted 4 March 2011
Available online 1 April 2011

Keywords:
Nanoparticle
Anti-reflection
Solar cell
External quantum efficiency

ABSTRACT

In this study, silica nanospheres dispersed in a surfactant solution were spin-coated on commercially available silicon solar cells to form colloidal crystals on the surface. This self-assembled nanoparticle layer served as an anti-reflection (AR) layer for solar cell devices. The self-assembled layer exhibits excellent anti-reflection properties in the UV and NIR wavelength regions, and the reflectance spectra match the theoretical prediction done using the rigorous coupled-wave analysis model. We also showed that the overall conversion efficiency of polycrystalline Si solar cells coated with the silica nanospheres was increased from 11% to 12.3% when using optimized spin-coating parameters and nanoparticle concentrations.

1. Introduction

Silicon (Si) is the leading material used in the commercial production of low-cost solar cells. The development cost of solar cells can be further reduced by either reducing the manufacturing costs or by increasing the solar cell efficiency. Various cost-competitive, relatively cheaper processing steps have been developed to make these solar cells more energy efficient. Due to the fact that nanoparticles have the characteristics of light harvesting [1–4], plasmon resonances and enhanced scattering [5], an appropriate and well-operated application of nanoparticles on the solar cells can therefore lead to high cell utility efficiency and provide low-cost production. Various solar cell substrates with nanoparticle deposits have been confirmed to enhance photocurrent [6] and acceptance angles [7] and improve the reflection of a specific wavelength (700–1100 nm) [8].

Recently, the scattering of incident light by nanoparticles has enabled the improved transmission of photons into the semiconductor active layers and the coupling of normally incident photons into the lateral, optically confined paths within the multiple-quantum-well waveguide layer, resulting in increased photon absorption, photocurrent generation, and power conversion efficiency of the solar cells [6]. Improvements in short-circuit current density (J_{sc}) have also been observed in quantum dot solar cells using silica and Au nanoparticles [8]. The scattering provided by the nanoparticles is believed to be essential for coupling and partially trapping light in substrate radiation modes. Although metallic nanoparticles provide efficient light scattering through coupling with surface plasmons, they exhibit extraordinary absorption at the surface plasmon resonances [9], significantly decreasing the overall effect of the metallic nanoparticles [10,11]. Other than the metallic nanoparticles, dielectric nanoparticles with high dielectric permittivity can also be an alternative for sufficient light scattering. More importantly, some of the dielectric materials possess a relatively low dissipation level at visible wavelengths. Recently, the use of dielectric nanoparticles has been demonstrated theoretically to lead to similar and even higher enhancements compared to that of metallic nanoparticles [12].

Most of the previous research presented good nanoparticle performance with regard to flat-surface of devices. However, there is no report on the fabrication or tests on the properties of the textured surface of Si-based solar cell devices incorporated with self-assembled dielectric nanoparticles. In this paper, we report a comprehensive study of the nanoparticle-enhanced performance of poly-silicon solar cells using dielectric nanomaterial (silica nanospheres) with particle sizes ranging from 100 to 500 nm. Nanoparticle colloidal crystals were fabricated on the solar cell surface to achieve the optimum anti-reflection property by controlling the spin rate, spin duration, and particle concentration on a custom-built spin coater. Optical properties of the self-assembled nanoparticle layers were also simulated based on the rigorous coupled-wave analysis (RCWA) method. The simulation results were compared with the experimental results.

2. Experimental section

In this study, the poly-Si solar cell was prepared by following commercial fabrication processes. The p-type Si wafers were

* Corresponding author.
E-mail address: kwsun@mail.nctu.edu.tw (K.W. Sun).

0927-0248/$ - see front matter © 2011 Elsevier B.V. All rights reserved.
doi:10.1016/j.solmat.2011.03.006

roughened using HF and HNO_3 and showed damaged etch with no additional texturization. A 200 nm n-type layer was created on the texture by $POCl_3$ diffusion using a centrotherm tube furnace to form the p–n junction, followed by the deposition of a thin anti-reflection layer of 80 nm SiN_x using a centrotherm direct plasma PECVD furnace. The front and rear side finger and bus bar contacts were screen-printed with a standard, commercially available lead containing Ag paste, Al paste, and Ag+Al paste using a semi-automatic ATMASC 25PP printer. The cells were fired using a fast firing conveyor belt furnace at an optimal firing temperature of 850 °C to make the fingers and bus bars come into contact with the N- and P-type regions for maximum performance. Finally, the cell edges were isolated using a 532 nm Nd:YAG laser cutting tool. The thickness of the entire poly-Si layer (p–n layer) and the metal contacts are 200 and 30 μm, respectively. The experiments and simulations in this report are all carried out on un-encapsulated cells.

The schematic of the device structure with the self-assembled Silica nanoparticles (SNPs) is shown in Fig. 1(a) and (b). SNPs purchased from the Golden Innovation Corp. with diameters of 100, 250, and 500 nm were first dispersed in a surfactant (mixture of EG/ethanol/DI with a ratio of 35:35:30 by volume) to make a 10 wt% suspension solution. The nanoparticles were patterned on top of the commercially processed poly-Si solar cells, mentioned above, with a light absorption area of $1.5 \times 1.5\ cm^2$ using a custom-made spin coater. The spin-coating process began at a spin rate of 350 rpm for 1 min, followed immediately by a faster spin rate of 3500 rpm for 30 s. The SEM image in Fig. 2 indicates that the nanoparticles self-assembled into closely packed structures on the cell surface because of the Van der Waals force [13] when the spin rates and the concentration of the SNP suspension solution in the recipe were properly adjusted.

All the solar cell devices with and without the SNP treatment were evaluated at room temperature based on the illuminated current density versus voltage (J–V) characteristics, the external quantum efficiency (EQE), and the reflectance. The photocurrent was analyzed using a solar simulator under the Air Mass 1.5 Global (AM 1.5G) illumination condition (100 mW/cm^2, 25 °C). The

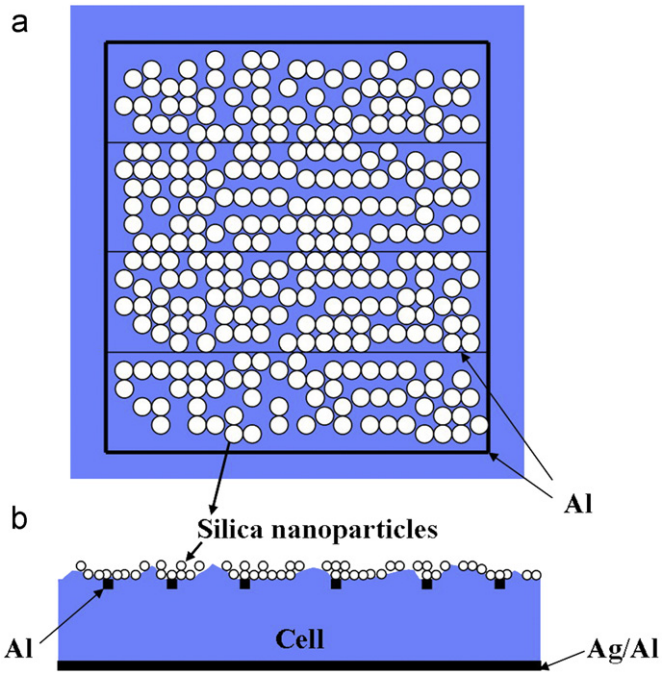

Fig. 1. (a) Schematic of the top view from a poly-Si solar cell with silica nanoparticles coated on the light illuminating surface ($1.5 \times 1.5\ cm^2$) and (b) side view of the device.

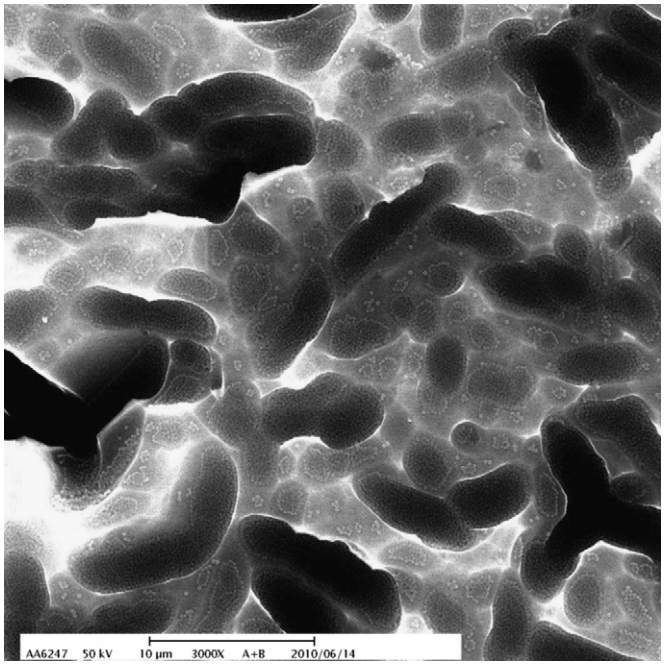

Fig. 2. SEM image of the self-assembled SNPs on the textured solar cell surface.

EQE was measured using an AM 1.5G standard spectrum and an Optosolar simulator (SR-150). The reflectance spectra of the samples were recorded using a UV–vis–NIR spectrophotometer (Hitachi U-4100) for wavelengths ranging from 200 to 1200 nm.

3. Results and discussion

The enhanced light absorption, and hence the efficiency of light scattering into the silicon active layer, depends on the nanoparticle diameter, percentage surface coverage, and material permittivity. Based on earlier reports [11,12] on maximizing the photocurrent response of solar cells, to achieve the best anti-reflection property from the self-assembled SNPs, there should be certain combinations of the diameter and areal density of the SNPs. To determine the best combination, we experimented on SNPs with diameter values of 100, 250, and 500 nm and with different areal densities of SNP done by controlling the nanoparticle dose (i.e., 125, 250, 500, and 1000 μl, respectively).

Fig. 3(a) and (b) shows the enlarged SEM images of the self-assembled SNP with particles sizes of 100, 250 and 500 nm, respectively, at a fixed dose of 1000 μl. As shown in Fig. 3(a), the SNP with a size of 100 nm formed a monolayer coverage throughout the entire textured surface. For the 250 nm SNPs, the self-assembled structure was monolayered near the top of the textured surface, but it had a multilayered structure at the bottom. However, for the 500 nm SNPs, the textured surface was almost filled by those particles due to their larger size. The flatter surface also increased the reflectance, which will be discussed later. As the particle dose was increased beyond 1000 μl, the surface became semi-opaque.

The maximum enhancement of the absorbed power in the poly-Si solar cells obtained after optimization of the size and surface coverage of SNPs is given in Fig. 4. The best overall power conversion efficiency, η, increased from 11% to 12.3%. The increase in conversion efficiency of the solar cells with the SNP treatment were 1.3%, 0.85%, and 0.6% for the 100, 250, and 500 nm sizes, respectively, at a dose volume of 250 μl. The efficiency increase of 1.3% was achieved when the solar cell

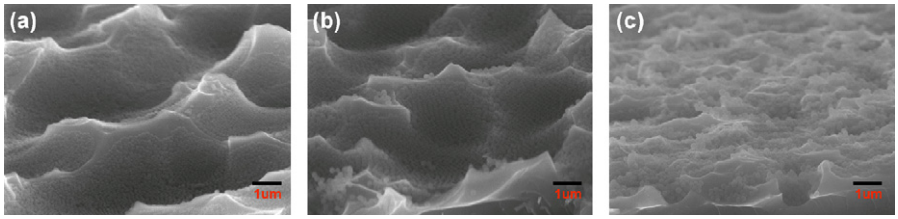

Fig. 3. Enlarged SEM images of the deposited SNPs on textured surface of cell with particle sizes of (a) 100 nm, (b) 250 nm, and (c) 500 nm at a nanoparticle dose of 1000 μl. The areal densities are $\sim 2.51 \times 10^{13}$, 1.61×10^{12}, and 2.01×10^{11} cm^{-2} in (a), (b), and (c), respectively.

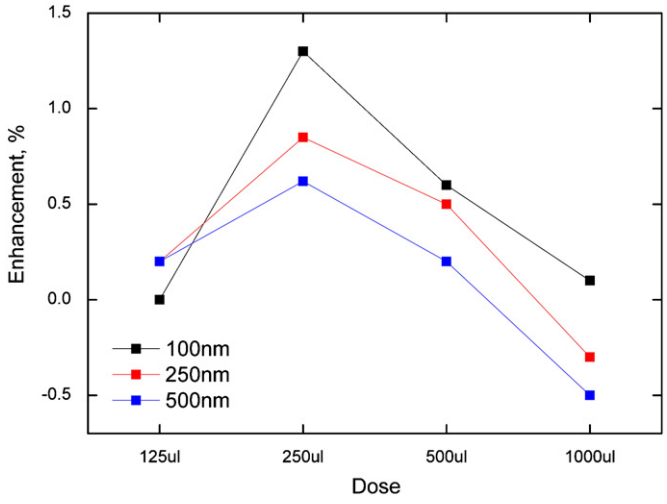

Fig. 4. Gains in conversion efficiency of poly-silicon solar cells after optimizing the size and coverage of SNPs.

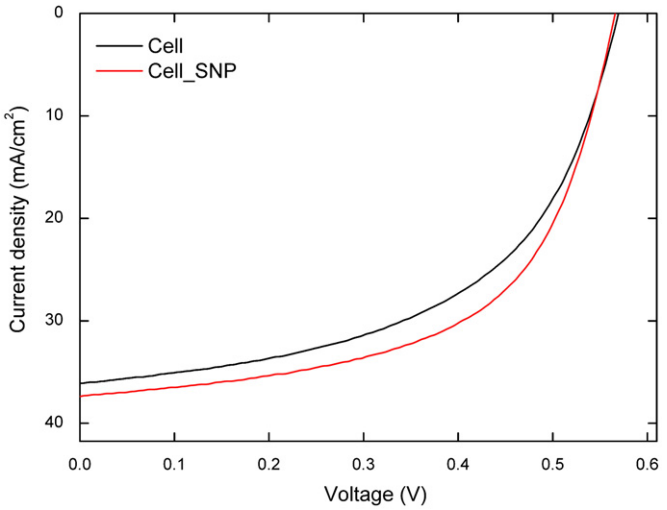

Fig. 5. *J–V* characteristics of the solar cells coated with the 100 nm SNPs compared to devices without the nanoparticles.

surface was covered with a monolayer of 100 nm silica nanoparticles with an areal density of around $1.1 \times 10^{13}/cm^2$. However, the enhancement factors began to drop when the nanoparticle dose was increased. This phenomenon was attributed to the substantial accumulation of nanoparticles, which eventually led to the self-assembled multilayer structures and flatter surface of the cell.

Fig. 5 shows the current–voltage (*J–V*) characteristic of the solar cell at maximum enhancement. The performance of the cell without the SNP treatment is also presented in parallel, for comparison. The short-circuit current density (J_{sc}), open-circuit voltage (V_{oc}), fill factor (FF), and conversion efficiency for the experiment cells are 37.4 mA/cm^2, 0.56 V, 0.58, 12.3% and, for the reference cells are 36.1 mA/cm^2, 0.57 V, 0.53, and 11%, respectively. In the figure, the J_{sc} increased from 36.1 to 37.4 mA/cm^2 with the 100 nm SNPs deposited on the textured surface. Note that the V_{oc} and FF remained almost unaffected. Therefore, the enhancement of cell efficiency is most likely due to the increase in photocurrent and light absorption. The reflectance spectra of the solar cells coated with SNPs of different sizes for maximum enhancement are plotted in Fig. 6. The reflectance spectrum of cells without SNPs is also displayed in parallel for comparison. The reflectance was reduced in the UV and IR regions for cells coated with self-assembled SNPs, whereas the change in reflectance in the visible region was insignificant. The EQE of the poly-Si solar cells coated with different sizes of self-assembled SNPs were measured relative to the cells without the SNP treatment, as shown in Fig. 7. Clearly, the increase in photocurrent is due to the enhanced absorption of light in the UV and the NIR regions by the active layer. The EQE measurements are in agreement with the reflectance results that light harvesting is improved in the wavelength ranges of UV and NIR due to the enhanced scattering by the self-assembled SNPs. In the best case, the EQE of the poly-Si solar

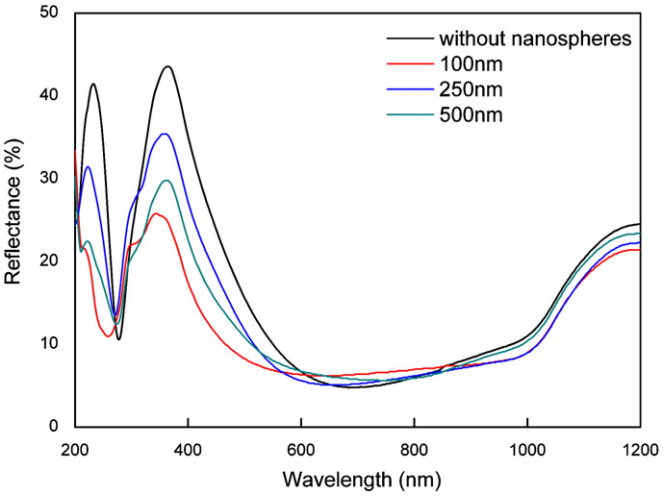

Fig. 6. Reflectance spectra of solar cells at maximum performance with coated particle sizes of 100, 250 and 500 nm. Spectrum of an untreated device is also presented for comparison.

cells was improved by over 40% and 56% in the UV and the NIR regions, respectively.

To compare with the experimental results, we simulated the surface reflectance of the cells using the RCWA method based on a three-dimensional model built according to the parameters used in this experiment and in the SEM images. The dimensions of the simulated solar cell structures and parameters used in the simulation are shown in Fig. 8. The deposited SNPs were assumed to be spherical, close-packed, and distributed in a square

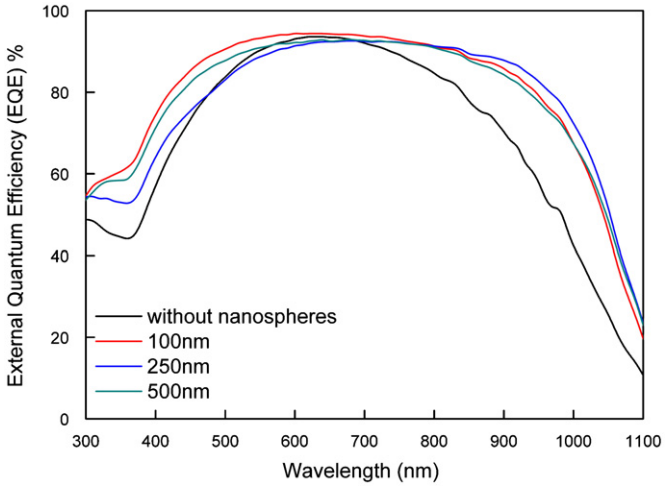

Fig. 7. External quantum efficiency measured under AM 1.5G illumination for solar cells at maximum performance with coated particle sizes of 100, 250, 500 nm, and untreated.

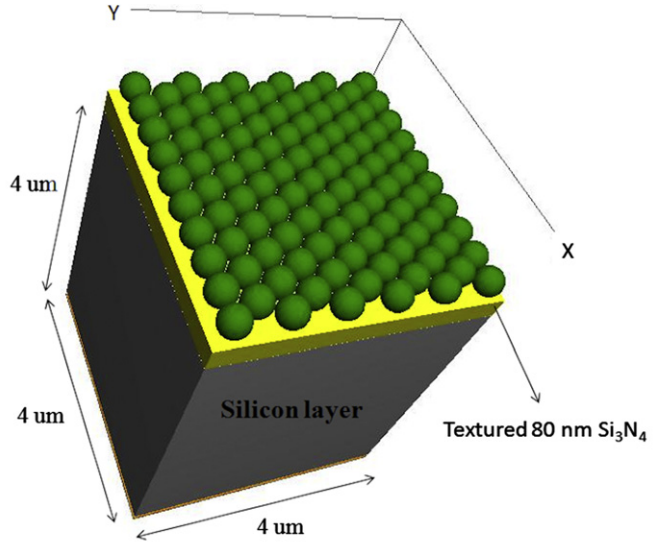

Particle size	100 nm	250 nm	500 nm
Areal density(cm^{-2})	$1.1*10^{13}$	$7.06*10^{12}$	$8.81*10^{11}$
Percentage of areal coverage(%)	86.39	34.65	17.29

Fig. 8. Schematic and table in the inset give the dimensions of the simulated device structures and parameters used in the RCWA calculations.

arrangement on top of the SiN_x layer. Periodic and matched electromagnetic boundary conditions were applied to the model to account for multiple scattering and cross-coupling of nearby nanoparticles. Reflectance of the solar cell was computed over the AM 1.5G spectrum, and the subsequent normalization of the value was calculated for the reference surface without SNPs. The comparisons between measurements and simulations in the UV and the NIR regions are shown in Figs. 9 and 10, respectively. The simulated reflection of the surface coated with SNPs agrees reasonably well with the experimental spectrum results.

A simple interpretation of our findings is given as follows: the scattering cross-section (σ_{sca}) and the absorption cross-section (σ_{abs}) of a sub-wavelength spherical particle can be written as [12]

$$\sigma_{sca} = \frac{1}{6\pi}(2\pi/\lambda)^4|\alpha|^2 \quad \text{and} \quad \sigma_{abs} = 2\pi/\lambda \mathrm{Im}(\alpha),$$

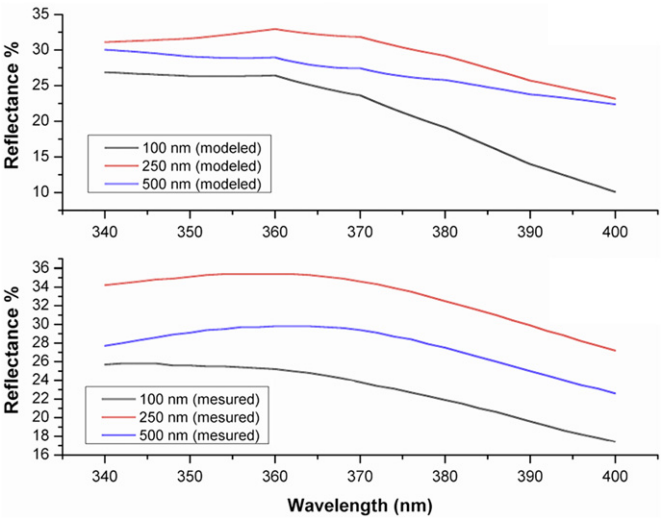

Fig. 9. Comparison of the simulated and measured reflectance spectra of the SNP treated solar cells in the UV region.

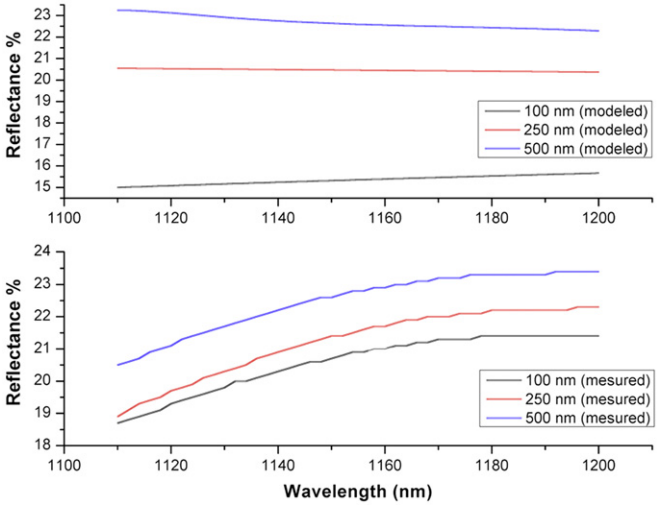

Fig. 10. Comparison of the simulated and measured reflectance spectra of the SNP treated solar cells in the NIR region.

where $\alpha = 4\pi R^3((\varepsilon-1)/(\varepsilon+2))$ is the polarizability of the particle. The particle polarizability, α, contains the size of the nanoparticle and the dielectric function. Higher order dipoles appear in nanoparticles as the particle size grows and the dielectric function changes. Therefore, the scattering cross-section of nanoparticles increases with the larger volume and dielectric function. Although the 500 nm particle has the largest polarizability among the three due to its larger size. However, in the UV region, the 100 nm particles are better "seen" by the shorter wavelength and have more chances to scatter light. Therefore, the surface coated with 100 nm particles shows the lowest reflection because the σ_{sca} is dominated by the factor $(1/\lambda)^4$. The monolayer distribution of the 100 nm particles also contributes to the reduced surface reflection. In the NIR region, the σ_{sca} is determined by the morphology of nanoparticle distribution because the wavelength is no longer a dominant factor. Again, SNPs of 100 nm diameter with a monolayer distribution give the lowest reflectance than those with multilayered structures.

4. Conclusions

In conclusion, we investigated the effects of dielectric scattering on absorption and photocurrent collection in the poly-Si solar cells

decorated with self-assembled SNPs. With optimized nanoparticle parameters, such as size and surface coverage, enhanced light absorption in the UV and the NIR regions were observed. The power conversion efficiency of the poly-Si solar cell increased by 11.8% when 100 nm SNPs with a monolayer distribution were deposited on the textured surface of the cell. Our numerical modeling also showed that SNPs deposits could significantly reduce surface reflectance in the UV and IR regions. Silica has the property of excellent thermal shock resistance and is chemically inert to most elements and compounds. The combination of strength, thermal stability and UV transparency makes it an excellent coating material under outdoor light-exposure conditions. This technology provides a true low-cost method for AR applications in solar cells to improve light harvesting efficiency.

Acknowledgment

This work was partially supported by the Bureau of Energy in Taiwan and National Science Council of Republic of China under Contract no. NSC 99-2119-M-009-004-MY3.

References

[1] D. Derkacs, S.H. Lim, P. Matheu, W. Mar, E.T. Yu, Improved performance of amorphous silicon solar cells via scattering from surface plasmon polaritons in nearby metallic nanoparticles, Applied Physics Letters 89 (2006) 093103-1-093103-3.

[2] D.M. Schaadt, B. Feng, E.T. Yu, Enhanced semiconductor optical absorption via surface plasmon excitation in metal nanoparticles, Applied Physics Letters 86 (2005) 063106-1-063106-3.

[3] S.H. Lim, W. Mar, P. Matheu, D. Derkacs, E.T. Yu, Photocurrent spectroscopy of optical absorption enhancement in silicon photodiodes via scattering from surface plasmon polaritons in gold nanoparticles, Journal of Applied Physics 101 (2007) 104309-1-104309-7.

[4] S. Pillai, K.R. Catchpole, T. Trupke, M.A. Green, Surface plasmon enhanced silicon solar cells, Journal of Applied Physics 101 (2007) 093105-1-093105-8.

[5] H.R. Stuart, D.G. Hall, Absorption enhancement in silicon-on-insulator waveguides using metal island films, Applied Physics Letters 69 (1996) 2327–2329.

[6] D. Derkacs, W.V. Chen, P.M. Matheu, S.H. Lim, P.K.L. Yu, E.T. Yu, Nanoparticle-induced light scattering for improved performance of quantum-well solar cells, Applied Physics Letters 93 (2008) 091107-1-091107-3.

[7] C.-P. Chen, P.-H. Lin, L.-Y. Chen, M.-Y. Ke, Y.-W. Cheng, J. Huang, Nanoparticle-coated n-ZnO/p-Si photodiodes with improved photoresponsivities and acceptance angles for potential solar cell applications, Nanotechnology 20 (2009) 245204 (1–6).

[8] C.O. McPheeters, C.J. Hill, S.H. Lim, D. Derkacs, D.Z. Ting, E.T. Yu, Improved performance of In(Ga)As/GaAs quantum dot solar cells via light scattering by nanoparticles, Journal of Applied Physics 106 (2009) 056101-1-056101-3.

[9] C.F.B.a.D.R. Huffman, Absorption and Scattering of Light by Small Particles, Wiley-Interscience, New York, 1983, 369-377.

[10] K. Nakayama, K. Tanabe, H.A. Atwater, Plasmonic nanoparticle enhanced light absorption in GaAs solar cells, Applied Physics Letters 93 (2008) 121904-1-121904-3.

[11] Y.A. Akimov, W.S. Koh, K. Ostrikov, Enhancement of optical absorption in thin-film solar cells through the excitation of higher-order nanoparticle plasmon modes, Optics Express 17 (2009) 10195-10205.

[12] Y.A. Akimov, W.S. Koh, S.Y. Sian, S. Ren, Nanoparticle-enhanced thin film solar cells: metallic or dielectric nanoparticles?, Applied Physics Letters 96 (2010) 073111-1-073111-3.

[13] Y. Lalatonne, J. Richardi, M.P. Pileni, Van der Waals versus dipolar forces controlling mesoscopic organizations of magnetic nanocrystals, Nature Materials 3 (2004) 121–125.